

Surface Constraints on Cr(VI) Incorporation into Calcite

R. Reeder, M. Nugent (SUNY, Stony Brook) and A. Lanzirotti (U. Chicago)

Abstract No. Reed1631

Beamline(s): X26A

Introduction: Hexavalent chromium, occurring as CrO_4^{2-} , is a serious environmental contaminant. This species is characterized by high mobility in soils and aquifers partly because of its weak interaction with mineral surfaces. Recent studies have shown that uptake of CrO_4^{2-} by coprecipitation with calcite may be enhanced significantly by rapid crystallization, such as may be found during wetting/drying or evaporative conditions. Previous studies of metal coprecipitation with calcite have shown that surface structure and microtopography may also influence the efficiency of incorporation during growth.¹ Calcite typically grows from aqueous solutions via the BCF mechanism on its dominant face ($10\bar{1}4$). Growth spirals are observed to form polygonized hillocks composed of two sets of symmetrically nonequivalent vicinal faces, each composed of identical monolayer growth steps.¹ Because these growth steps are structurally distinct, the extent of metal incorporation may vary between adjacent vicinal faces by as much as a factor of 10. This has a significant influence on the overall effectiveness of Cr(VI) uptake. We have used micro-XRF to evaluate the surface structural influence on CrO_4^{2-} incorporation in calcite.

Methods and Materials: Calcite single crystals were synthesized in room-temperature aqueous solutions using methods reported elsewhere.¹ Crystals were dominated by the ($10\bar{1}4$) face, which uniformly exhibit polygonized growth hillocks consistent with the *c*-glide surface symmetry element. Sections were made parallel to an individual growth face to allow micro-XRF analysis of the surface-most portion of the face containing the vicinal flanks of the spiral. Micro-XRF at X26A used a 15 x 15 μm monochromatic X-ray beam combined with a solid-state detector to determine the spatial distribution of Cr incorporated at the growth surface.

Results and Conclusions: The observed spatial distribution of Cr corresponds exactly to the pattern of the structurally nonequivalent regions of the growth surface (Fig. 1). This is readily seen by a line analysis that traverses adjacent nonequivalent vicinal faces (Fig. 2). Cr incorporation is greatest in the region labeled A and lowest in B. The concentration difference is a direct record of the uptake preferences between the different growth step arrays of the vicinal faces: approximately 220 ppm in A and 60 ppm in B, giving a differential incorporation factor of 3-4. It is notable that CrO_4^{2-} is preferentially incorporated into vicinal region A. In contrast, a previous study by Staudt et al.² found that SO_4^{2-} and SeO_4^{2-} , also having tetrahedral geometry, were preferentially incorporated into vicinal face B. The cause for the growth step-selective incorporation has been attributed to differences in surface site geometry between the nonequivalent steps in the different vicinals. However, the difference in behavior between CrO_4^{2-} and SO_4^{2-} and SeO_4^{2-} remains unclear. Nevertheless, the findings demonstrate that the presence of multiple, structurally distinct surface sites influences Cr(VI) uptake behavior by calcite. And the spatial segregation of these sites on the surface during spiral growth suggests that uptake during natural crystallization of calcite may be heterogeneous.

References: ¹ R.J. Reeder, "Interaction of divalent cobalt, zinc, cadmium, and barium with the calcite surface during layer growth," *Geochimica et Cosmochimica Acta*, **60**, 1543, 1996. ² W.J. Staudt, R.J. Reeder and M.A.A. Schoonen, "Surface structural controls on compositional zoning of SO_4^{2-} and SeO_4^{2-} in synthetic calcite single crystals," *Geochimica et Cosmochimica Acta*, **58**, 2087, 1994.

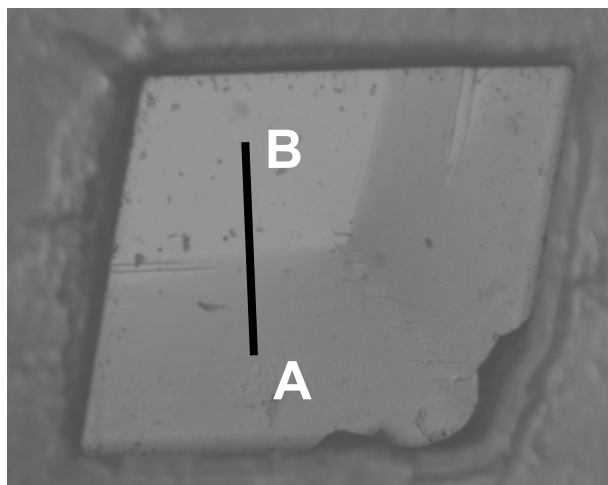


Figure 1. Differential interference contrast image of an as-grown $10\bar{1}4$ face of calcite showing a single polygonized growth hillock indicated by the different shading patterns.

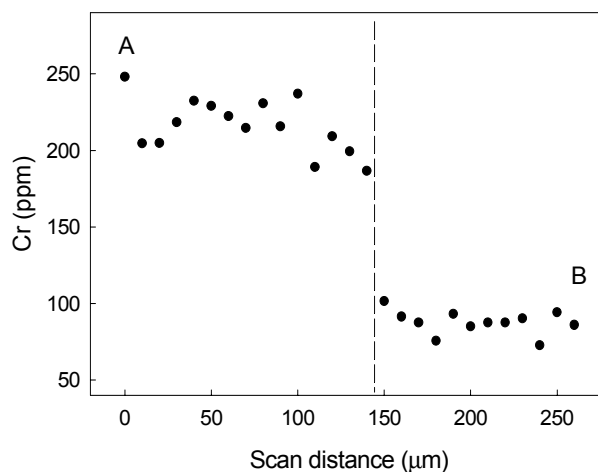


Figure 2. Micro-XRF line scans traversing adjacent non-equivalent vicinal faces labeled A and B.